The International Journal of Advanced Manufacturing Technology (2023) 127:3195–3207
https://doi.org/10.1007/s00170-023-11350-z

ORIGINAL ARTICLE

Influence of shielding gas coverage during laser hot-wire cladding with high carbon steel

Laura Budde[1] · Kai Biester[1] · Timm Coors[2] · Mohamad Yusuf Faqiri[3] · Marius Lammers[1] · Jörg Hermsdorf[1] · Thomas Hassel[3] · Florian Pape[2] · Ludger Overmeyer[1,4]

Received: 18 November 2022 / Accepted: 28 March 2023 / Published online: 10 June 2023

Abstract
In contrast to conventional components made from a single material, hybrid multi-material components allow the production of load-adapted parts with different materials in different structural and functional areas. Hardenable and forgeable steels with a high carbon content are suitable for increasing fatigue and wear resistance and thus an extension of component life. However, materials with an equivalent carbon content of more than 0.6 are considered difficult to weld due to their tendency to crack. This study investigates the influence of the shielding gas coverage on the laser hot-wire cladding process with high carbon cladding material AISI 52100. For this reason, welding tests were carried out with different parameter combinations in a process chamber flooded with argon. The oxygen content in the chamber was less than 500 ppm during the welding process. The claddings welded in the process chamber are compared to the claddings welded in a previous investigation with a commercial shielding gas nozzle for laser deposition welding with wire. The tests conducted showed reduced pore formation and very little sparking. By using a process chamber, the average degree of dilution was reduced from 16.9% to 8.5% and burn-off of alloying elements was reduced. In most cases, high hardness values of 700 HV0.1 to 850 HV0.1 were achieved. The use of the process chamber demonstrates that the shielding gas coverage and therefore the remaining oxygen content have a high influence on the process stability and seam quality when welding high carbon steel. Such a considerable effect has not yet been observed with other commercially available cladding steels.

Keywords LHWC · Cladding · High carbon steel · Shielding gas · AISI 52100

1 Introduction

Technical applications cause loads in machine elements that place different or even opposing requirements on the local material properties. Locally different requirements on a component can be harmonized by claddings with load-adapted material areas. By using different deposition welding processes, it is possible to weld fatigue- and wear-resistant surfaces onto easily machinable and ductile base materials [1, 2]. In addition to hardness, strength, corrosion resistance and density, the local component geometries (shape and position of the joining zone) and the material purity of the material of the cladding are crucial for the application behavior of the component. Many applications require high-strength hardness materials to meet wear resistance and fatigue requirements. For these applications, hardenable and forgeable steels with high carbon content are used. However, these steels are considered difficult to weld due to their high carbon content and the resulting increased tendency for cracks.

Welding of steel with a high carbon content is only possible with great effort such as preheating the substrate or is not possible at all due to poor weldability. Defects can occur in various forms such as cracks or pores. The high carbon content in combination with alloying elements leads to hardening and embrittlement in the heat-affected zone. Lower ductility is caused by the increased brittleness, resulting in an increased risk of material defects. During laser cladding, high cooling rates occur, increasing the before mentioned effect by forming a microstructure with high lattice stresses, consisting of martensite [3]. As a result of the difficulties in welding high carbon steels, these materials have rarely been used for additive manufacturing or deposition welding. The high carbon tool steel Fe85Cr4Mo8V2C1 with a carbon content of

✉ Laura Budde
l.budde@lzh.de

Extended author information available on the last page of the article

1% was investigated in a laser powder bed fusion (L-PBF) process by Sander et al. The base plate was preheated to a temperature of 500°C and the process chamber was flooded with argon. Two sets of parameters were determined for components with a density greater than 99.6%. Compared to the as-cast condition with a compressive strength of 3500 MPa and a hardness of 743 ± 12 HV0.1, a higher compressive strength of 3796 ± 163 MPa and a higher hardness of 900 ± 12 HV0.1 were obtained for the specimens manufactured by the L-PBF process [4].

M2 HSS powder with a carbon content of 0.9% was used by Kempen et al. in a similar setup with the L-PBF process. The study showed that preheating the base plate prevented delamination of the weld structure from the base plate and cracks in the structure. By preheating the base plate to a temperature of 200°C, a maximum density of 99.8% could be achieved. By remelting after each applied layer, the hardness rose from 57 HRC to 64 HRC (about 630 HV to 800 HV). Heightened hardness can be attributed to the increase in the martensitic phase which enhances the tendency to crack formation [5]. In the investigation of the weldability of tool steel X110CrMoVAl8-2 by Feuerhahn et al. applying an L-PBF process, crack-free specimens with a homogeneous microstructure and only small pores could be produced. By a subsequent heat treatment of the specimens, an increase of the hardness with a value of 765 HV could be achieved [6].

Coors et al. investigated a new process chain for the production of hybrid axial bearing washers, consisting of deposition welding, hot forming, machining and heat treatment [7]. A cladding of AISI 52100 was applied to a substrate of AISI 1022M by plasma transferred arc welding. With subsequent hot forming, a reduction in the number of pores in the area of the bearing washer running surfaces was achieved and the microstructure was improved. After deposition welding and hot forming, a hardness of 400 HV0.5 to 500 HV0.5 was measured in the cladding. Through heat treatment, the hardness could be increased to 880 HV0.5, which corresponds to the hardness of conventional bearing washers used in industry. After deposition welding and hot forming, the microstructure consists mainly of pearlite. After heat treatment of quenching and tempering, a martensitic microstructure is present. Studies on the service life of the hybrid bearing washer showed a service life of 82% compared to the conventional bearing washer. Pores and voids are the reason for the reduced service life. Behrens et al. researched the mechanism of pore closure during hot forming of AISI 52100 claddings, performing compression tests on monomaterial and hybrid specimens. Closing the pores to a large extent required a plastic strain in the cladding material of 0.7 [8].

In addition to the previously mentioned powder-based processes, a laser hot-wire cladding (LHWC) process can also be used to manufacture claddings. The fundamental suitability of the process to produce claddings was proven by manufacturing of claddings of X45CrSi9-3. This material has a carbon equivalent of >2 due to the high carbon and chromium content. This research used a standard welding nozzle with shielding gas supply and there were no indications of insufficient shielding gas coverage [9, 10].

The application of shielding gases in laser welding is very important. Without shielding gases, pores and cracks can increasingly form, as the melt pool can absorb more oxygen, nitrogen and moisture. Therefore, optimum shielding gas coverage is mandatory to protect the process zone from environmental influences. The shielding gas can be supplied to the process zone through the welding nozzle or added through a separate nozzle. The basic requirement for achieving good shielding gas coverage is a laminar flow of the shielding gas from the nozzle to the workpiece. If the velocity is too high, the ambient atmosphere is drawn into the gas jet by turbulence and thus enters directly into the weld seam. The shielding gas can be supplied via various nozzles, including coaxial nozzles, lateral nozzles or annular gap nozzles. Various shielding gases are used in laser beam welding. In particular, the gases helium and argon are preferred. Argon is an inert gas that is heavier than air and does not react chemically with the material [2]. The selection of the right shielding gas depends on various factors. Of importance are the type of laser beam source and, associated with this, the wavelength used, the beam intensity and also the working temperature. In addition, the shielding gas depends on the base material used. For diode lasers, it is recommended to use argon or argon mixtures to protect the process zone. For non-alloy and low-alloy steels, argon or an argon mixture with a small amount of oxygen can be used. Nitrogen is often avoided, as this could lead to embrittlement or premature aging of the material. However, during laser metal deposition welding with duplex stainless steel wire, the use of nitrogen as shielding gas can lead to the avoidance of nitrogen loss in the deposited material [11]. If high-alloy steels are used, argon or an argon mixture with a lower hydrogen content should be used. The use of hydrogen can reduce tarnish colors [12].

Tapoglou, Clulow and Curtis conducted shielding gas coverage studies using multiple methods with a laser metal deposition with powder (LMD-P) process [13]. The common feature of the methods used is the use of a shielding gas chamber. Two of the methods differ in the delivery of the shielding gas, with the gas being injected only in the first variant and the gas being delivered diffuse in the second variant. The third variant uses the diffuse gas supply and an additional cover of the process chamber. Oxygen reactive material Ti6Al-4V and non-reactive materials Iconel 718 and 15-5 PH stainless steel were used. The results with stainless steel and Inconel showed that, compared to welding tests outside the chamber, oxidation was best reduced in the shielding gas chamber with cover. Residual oxygen values of 100 ppm could be achieved

using the method with cover. Titanium specimens were created in the shielding gas chamber with a low oxygen content of 0.079%.

Previously, such an argon process chamber was applied by Pape et al. for foaming titanium powder mixed with foaming agents using a diode laser, where oxygen contamination is very critical [14].

Guillen et al. investigated sparks ejected by grinding of steel and linked the steel microstructure to the splitting behavior of the spark, studying a steel with a carbon content of 0.17% and a hypereutectic steel with a carbon content of 1.15%. They observed sparks with a highspeed camera. Hypereutectic sparks showed various splitting behavior. Most sparks constantly emitted small sparks around them while some produce explosions. A common explanation for this is the diffusion of oxygen into the microstructure, which leads to the formation of carbon dioxide. The gas content increases until the pressure leads to a breaking of the spark. In a grinding experiment in a chamber filled with neon only very few dim sparks were observed. This indicates the influence of the oxidation on sparking [15].

In a previous study [16], the influence of the process parameters of laser power, current, wire feed rate, welding speed, and weld seam overlap on the dilution, pore formation, process stability, and waviness of an AISI 52100 cladding produced by LHWC was investigated. The investigations showed that simultaneous optimization of pore formation and dilution is not possible, as both show opposite tendencies. A low degree of dilution is associated with a high pore occurrence while a high degree of dilution is associated with a low pore occurrence. Two unusual effects occurred during the deposition welding experiments. Strong sparking was observed in some parameter sets. This was particularly the case at a high wire feed rate. Additionally, surface pores appeared in large numbers with some parameter sets. Therefore, the next step is to investigate whether insufficient shielding gas coverage caused the before mentioned effects and to what extent improved shielding gas coverage has an effect on the process.

In order to determine the influence of the shielding gas on the welding process and the resulting properties of the cladding, specimens welded with shielding gas supplied via the welding head will be compared with specimens from the process chamber flooded with pure argon. The use of the process chamber can ensure complete shielding of the melt pool from the ambient air. The following aspects will be investigated:

- Dilution
- Sparking during the welding process
- Pore occurrence
- Chemical composition of the cladding
- Process stability
- Hardness
- Microstructure

2 Materials and methods

Flat steel of austenitic stainless steel AISI 316L with a thickness of 10 mm is used as substrate for the experiments. A 1.0 mm diameter wire of bearing steel AISI 52100 is used as cladding material. Table 1 shows the chemical composition of both materials according to the manufacturer data sheet.

The 3.3 kW diode laser beam source LDM3000-40, manufactured by Laserline GmbH, is used for the experiments. The laser source has a wavelength of 1020–1060 nm ± 15 nm and a fiber core diameter of 400 µm. LHWC is performed using a coaxial welding head [17]. In this processing head, a reflectively coated pyramid splits the laser beam into four partial beams to be again recombined into a spot by means of deflection mirrors. The combination of a collimator with a focal length of 100 mm and a focusing unit with a focal length of 300 mm leads to a laser beam with a focus diameter of 1.6 mm. The stickout length of the wire is kept constant at 7 mm for the entire series of tests.

Figure 1 shows the experimental setup for LHWC on flat steel. The clamping device is mounted on an XY-axis. The substrates are fixed via four pneumatically operated clamping devices. The wire feed unit DIX FED 100L and the hot current source DIX PI 270, both manufactured by Dinse GmbH, are used to feed and preheat the wire.

During LHWC, current and wire feed rate signals are monitored. The signals are used to assess the process stability.

The process stability can be determined by different wire transfer modes [18], which can be distinguished with the help of the signal for the wire feed rate and the current for resistance heating. The wire transfer mode for the stable welding process is the smooth wire transfer. The modes, which describe unstable wire transfer are globular wire transfer and wire transfer by plunging. Figure 2 shows signals for all three wire transfer modes. For the smooth wire transfer mode, the actual signals for wire feed rate and current are within a tolerance range of ±5%, which is self-defined, around the set point. The tolerance limits are based on the signals at wire feed without process. Any values outside the tolerance range are not up to standard and the process is therefore classified as unstable. The wire transfer by plunging is characterized by a wire signal that fluctuates a lot and does not reach the setpoint constantly. This can be explained by the fact that the wire reaches the bottom of the melt pool, causing the wire to jam back. The current signal, on the other hand, is constantly within the tolerance range of the setpoint in this mode. The third wire transfer mode can be identified by the current signal, which is suddenly collapsing. This collapse is caused by the wire burning back and the electrical

Table 1 Chemical composition in wt.% of AISI 316L and AISI 52100 (according to manufacturer data sheets)

	Fe	C	Si	Mn	P	S	Cr	Ni	Mo	Co
AISI 316L	bal	0.022	0.516	1.583	0.037	0.0004	17.56	12.71	2.606	0.181
AISI 52100	bal	0.940	0.200	0.340	0.009	0.007	1.400	–	0.010	–

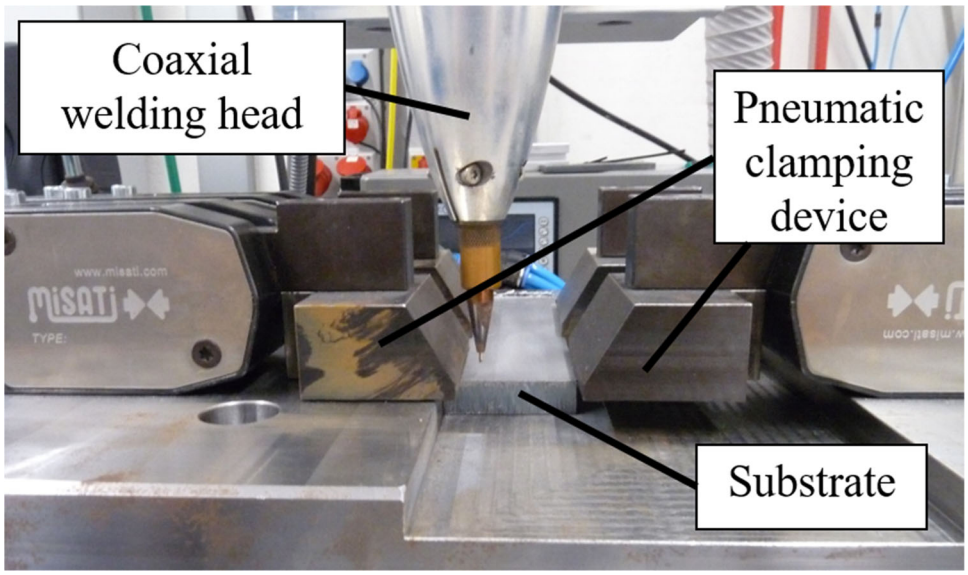

Fig. 1 Experimental setup for LHWC outside the process chamber

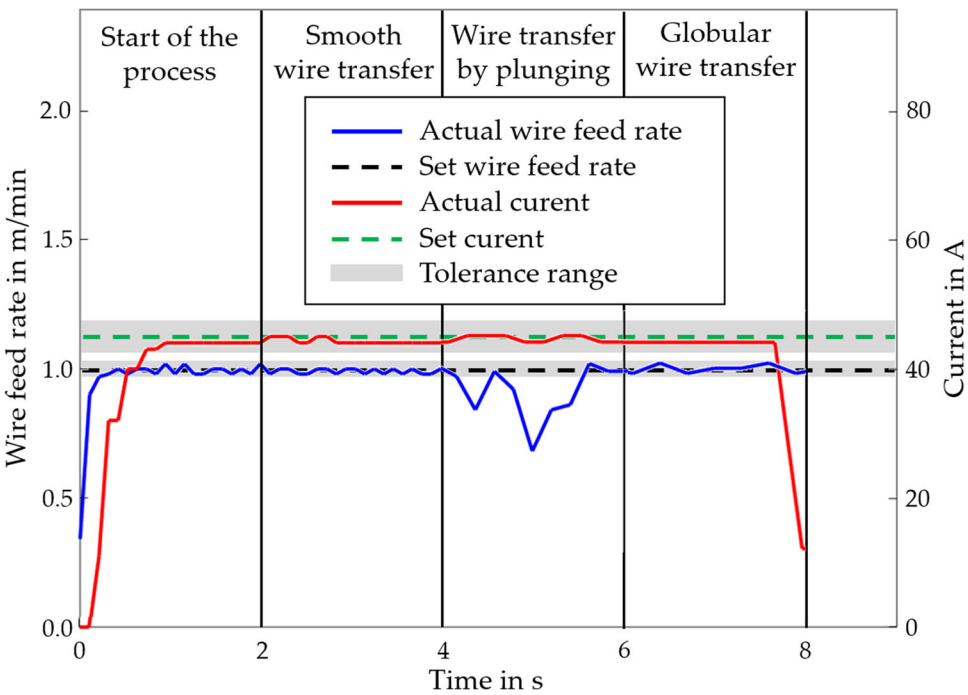

Fig. 2 Signals of wire feed rate and current at different wire transfer modes

current for resistance heating breaking off due to the lack of contact with the melt pool. In this mode, however, the signal for the wire feed is constantly within the tolerance range of the setpoint.

Figure 3 shows the experimental setup used for laser cladding in a process chamber. The process chamber enables the oxygen content to be reduced by flooding the chamber with the shielding gas argon. The oxygen sensor SGM7 from Zirox GmbH is used to measure the level of residual oxygen in the chamber. Due to the higher density argon displaces the ambient air upward, allowing the air to escape through the chamber, which is open at the top. Additional masking of the upper chamber area creates a minimal opening, minimizing argon loss during the process.

Based on previous investigations, this investigation selected six parameter sets, shown in Table 2. Two parameter sets were selected due to strong sparking, and two others due to strong pore formation. In addition, two parameter sets are investigated in which premature process termination occurred due to back-burning of the wire.

For each parameter set, the comparison is made between the process with a shielding gas supply of 8 l/min via the processing head and the process in the process chamber. This leads to a total of 12 different welding parameters. The cladding consists of eight seams, each 60 mm long, which are welded unidirectional. In order to investigate the chemical composition, the number of weld seams is increased to reach a total width of 20 mm. When cladding in a process chamber, the change of oxygen content is observed. The process starts at less than 100 ppm residual oxygen content, which increases to a maximum of 500 ppm during the process due increased temperature of the substrate and resulting gas turbulences.

Various properties of the cladding are determined to assess the influence of the shielding gas. The dilution is the ratio of the melted substrate to the applied material and melted substrate. In the cladding process, the aim is to achieve a minimal amount of dilution, since low dilution results in a high purity of the cladding material. With low dilutions, the desired properties of the cladding are already achieved in the first layer; otherwise, several layers have to be welded on top of each other.

To calculate the dilution, the substrates with the claddings are cut. Cross-sections are prepared by embedding the samples, polishing them and then etching them with the etchant Adler. To determine the areas needed for calculating the dilution, the micrographs are first taken with a VK-X1100 laser scanning microscope (Keyence GmbH) and then measured with the MultiFileAnalyzer software. Figure 4 shows the different areas on a cladding that are measured to determine the

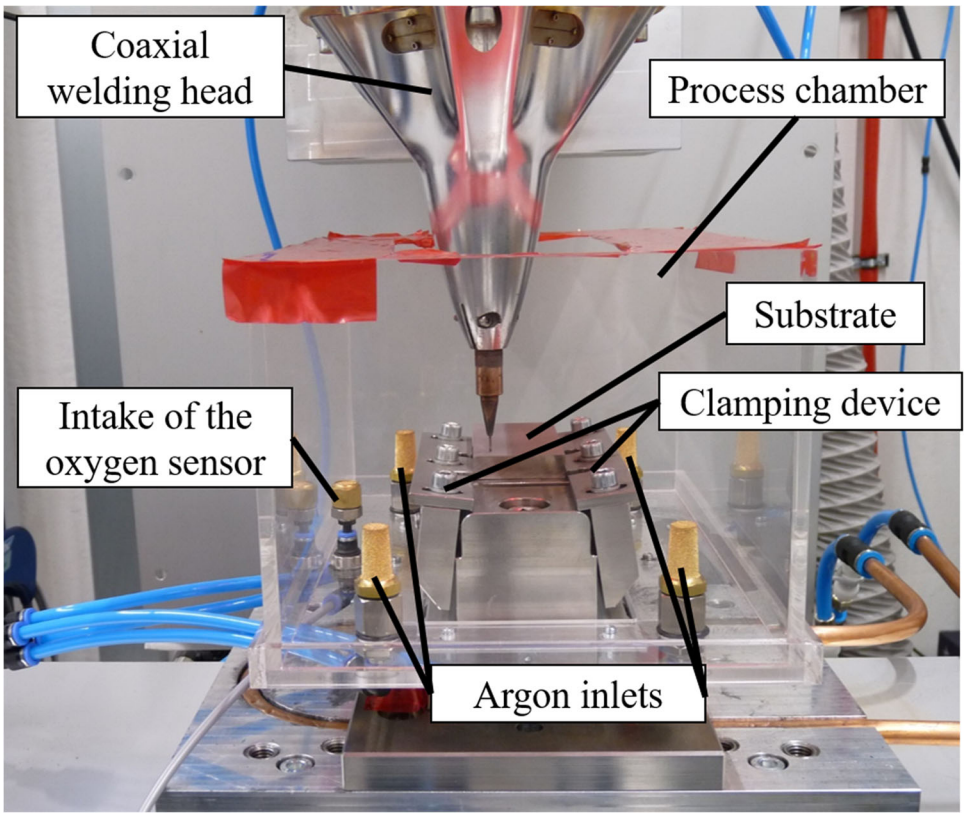

Fig. 3 Experimental setup for LHWC in a process chamber flooded with argon

Table 2 Examined process parameters

Number	Laser power in kW	Current in A	Wire feed rate in m/min	Welding speed in mm/min	Overlap in %	Examined according to
P1	1.9	75	2	1200	50	Pore occurrence
P2	2.1	60	2	400	20	Pore occurrence
S1	1.9	45	2	400	50	Sparking
S2	2.2	75	2	400	50	Sparking
PS1	2.2	75	1	1200	50	Pore occurrence
PS2	2.1	75	1	400	20	Pore occurrence

dilution. Equation 1 shows how the dilution d can be determined.

$$d = \frac{A_{melt}}{A_{clad} + A_{melt}} \cdot 100\% \quad (1)$$

A_{melt} indicates the area of the melted substrate and A_{clad} the area of the applied material.

Sparking occurs during welding. The reason for sparking can be incorrectly set welding parameters or insufficient shielding gas coverage. It is analyzed whether sparking can be reduced by welding in a process chamber by carrying out the same welding process with and without a process chamber.

In order to determine pore size and distribution ultrasonic measurements are performed on one sample per parameter set. Pape et al. have demonstrated that this method is well applicable for testing of samples made of multiple materials [19]. By analyzing the runtime signal for a certain runtime range, here a gate with a length of 25 ns, a 2D image can be generated by converting the runtime signal into greyscale. Thus, an acoustic horizontal section image is calculated. By measuring different gates in the z-direction, the specimen can be characterized layer wise, thus determining the exact location of material or welding defects. Ultrasonic testing is performed with a modified PVA TePla SAM 301 system. A transducer with a frequency of 30 MHz and a focus length of 12.7 mm was selected. The detection limit is 7 µm with an axial resolution of 14 µm.

The composition of cladding is determined with the spark spectrometer SPECTROMAXx (SPECTRO Analytical Instruments GmbH). A high-energy spark excitation ignites a plasma between the sample and the copper electrode in an argon atmosphere. This produces a light emission which is measured and assigned to the chemical elements. On each sample three measurements were taken.

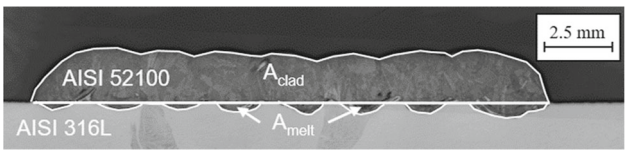

Fig. 4 Macrographic cross-section of a cladding of AISI 52100 marked with areas for determination of dilution

The microhardness measurement according to Vickers is carried out in accordance with DIN EN ISO 6507. HV0.1 is measured with a test force of 0.98 N and a test duration of 10 s. The course of the hardness over the entire weld seam is determined by measuring a series of measurements from the surface of the deposited material to the base material. For each parameter set, except for PS1 and PS2, two samples are analyzed with four measurement series. Hardness measurements were not carried out on those parameter sets, as not all planned measurement positions could be investigated on these samples due to the premature termination of the process, and comparability could therefore not be guaranteed. The measurement series are evenly distributed over the sample and each consists of 45 measurement positions with a spacing of 0.1 mm.

3 Results and discussion

The influence of a process chamber on the dilution of the cladding is shown in Fig. 5. Mean dilution of parameter sets P1-S2 for LHWC in a process chamber and with an argon flow rate of 8 l/min are compared.

The dilution is significantly reduced by welding in a process chamber. Without the use of a process chamber, a mean dilution of 16.9% can be achieved, while by cladding in a process chamber, a mean dilution of 8.5% is observed. The highest dilution of 25.9% is achieved in a cladding manufactured with parameter set P2 and a shielding gas flow rate of 8 l/min. The lowest dilution of 3.4% is achieved using parameter set S1 and using a process chamber. This indicates that the melt pool is not adequately shielded from the ambient air by the shielding gas flow during welding outside the process chamber. Due to the reaction with the ambient air, additional energy enters the process zone and leads to a stronger melting of the base material. The ratio of deposited material to melted

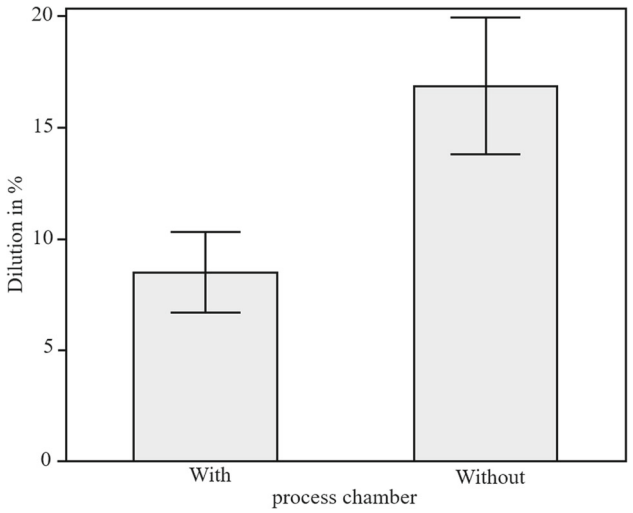

Fig. 5 Influence of shielding gas on mean dilution and confidence interval for LHWC of AISI 52100 on AISI 316L (P1-S2)

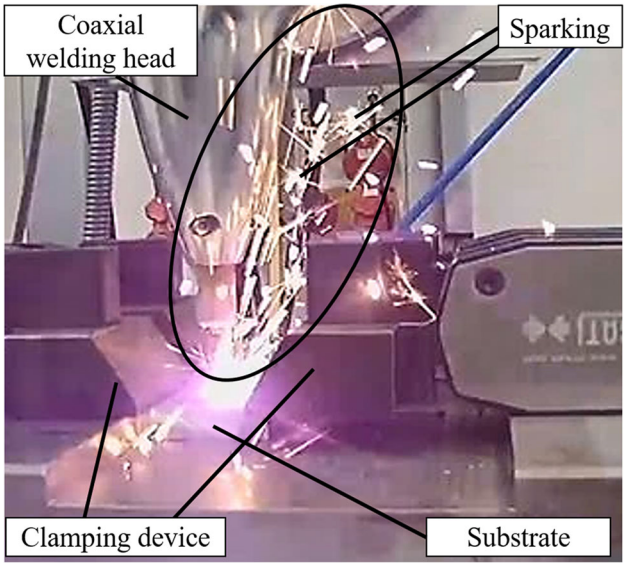

Fig. 6 Sparking during LHWC without a process chamber using welding parameter set S2

base material changes. Outside the process chamber, the still hot track can react with the ambient air after the process head has passed and an oxide layer is formed. When welding the next adjacent tracks, the oxide layer absorbs the laser radiation better than the steel surface of the substrate, resulting in a higher temperature on the existing track than on the steel substrate surface. This results in a higher degree of dilution due to the higher temperature.

During welding of some parameter sets, strong sparking occurs. Previous investigations have shown that the effect occurs especially at high wire feed rates of 2 m/min while at low wire feed rates of 1 m/min the sparking does not occur. Figure 6 shows the sparking during LHWC with a shielding gas flow rate of 8 l/min (parameter set S2). The appearance of the sparks is similar to those produced during grinding of high carbon steels [20].

In comparison, Fig. 7 shows the welding process in the process chamber with otherwise identical welding parameters. As expected based on the results of Guillen et al. [15], no sparking occurs. For both sets of parameters, which were previously prone to sparking, sparking could be suppressed by using the process chamber.

The previous investigation has shown that pore formation is a major challenge when welding AISI 52100. Surface pores and pores within the cladding appear in large number with some parameter sets. A cladding with strong surface pore occurrence is shown in Fig. 8. The cladding was manufactured using parameter set P1 with an argon flow rate of 8 l/min.

To investigate this further, non-destructive pore detection is carried out using a scanning acoustic microscope (SAM) in pulse-echo configuration. The surface of the cladding is ground parallel to the substrate surface and was subsequently polished. The samples were placed in a basin with distilled water as a coupling medium. For the two parameter sets where severe pore formation occurred (P1 & P2), the SAM measurements are compared in terms of pore number and distribution. The pores that form on the surface can be reduced by adjusting the laser beam profile. With a larger cross-sectional area of the laser radiation on the substrate with an adapted intensity distribution or laser power, the solidifying metal can remain in the molten state for longer, so that the melt can outgas and the surface pores can be reduced or prevented. Figure 9 shows the SAM images for samples of parameter set P1 when welding with and without a process chamber. The pore distribution at three different depths (0.6 mm, 1.0 mm and 1.5 mm below the surface) is shown.

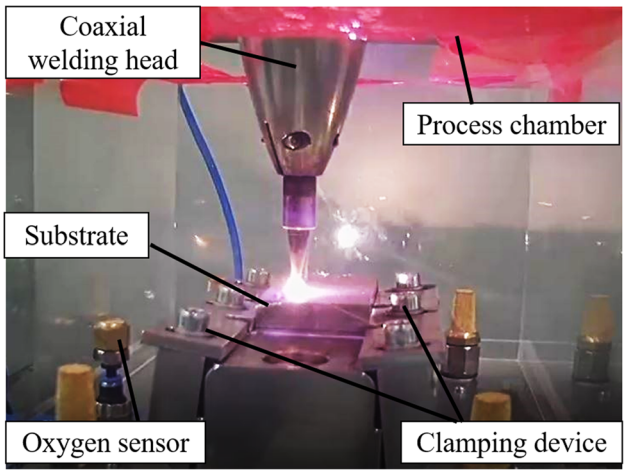

Fig. 7 LHWC process in a process chamber flooded with argon using parameter set S2

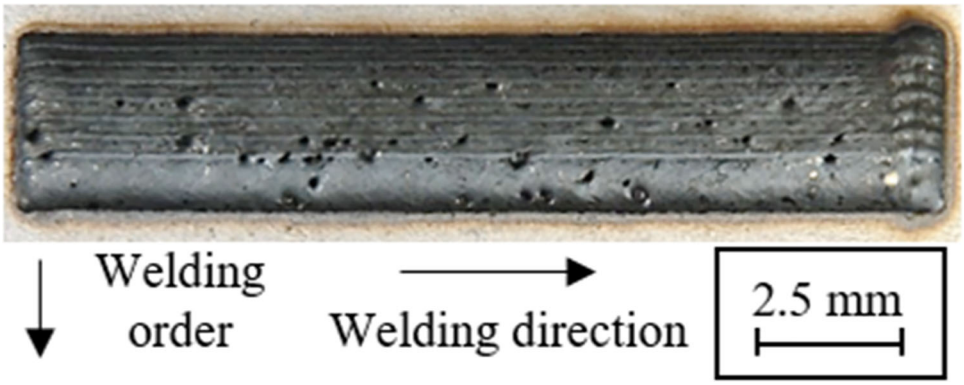

Fig. 8 Top view of a cladding manufactured outside a process chamber with a shielding gas flow rate of 8 l/min using welding parameter set P1

The white dots represent the pores in the sample. When comparing the two samples, it can be seen that the number of pores is remarkably reduced in the sample from the process chamber. However, pores still appear, especially in the area near the surface of the cladding.

In order to quantify the amount of pores, the pore densities in the respective layers were analyzed with the software ImageJ [21]. By adjusting the image threshold of the dark to white zones, the pore content in relation to the total area could be derived, see Fig. 10. As can also be seen in the SAM images, pore number decreases with greater depth near the substrate material. Overall, the test arrangement with process chamber shows an approximately three times lower density of pores.

The mean amount of alloying elements in the claddings of parameter sets P1 to S2 depending on shielding gas coverage is shown in Fig. 11. The values for the elements phosphorus and sulfur are not listed, since no valid statement is possible due to the low content. The mean weight percentage of the alloying elements is higher in claddings manufactured in the process chamber. This effect cannot be explained solely by the previously shown deviations in the degree of dilution. The higher degree of dilution can explain the lower carbon content (0.94% in the wire material and 0.022% in the base material) but not the deviations in the chromium and nickel content. With increasing dilution, due to the high chromium and nickel content of the austenitic base material, an increase of the corresponding proportions in the sample, which was subjected to 8 l/min argon gas flow rate, is expected. However, this is not the case.

This indicates that burn-off of alloying elements occurs during the welding process outside the process chamber, which is suppressed during welding in the process chamber. The difference in the carbon content is higher in parameter

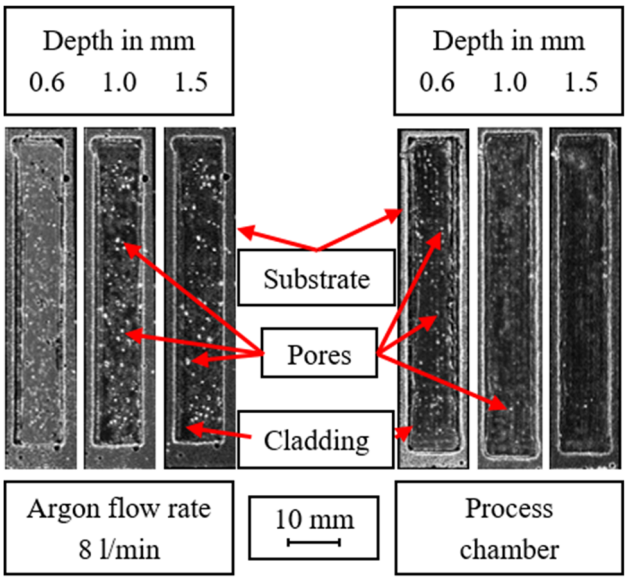

Fig. 9 SAM images for non-destructive detection and quantification of weld defects with and without a process chamber using weld parameter set P1

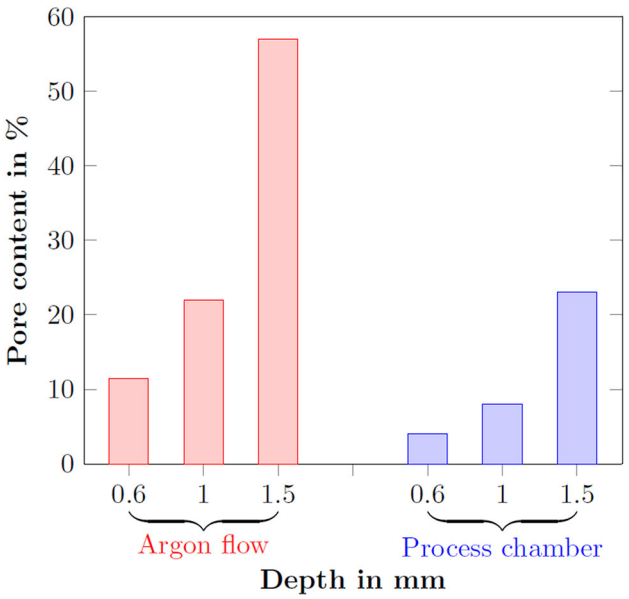

Fig. 10 Evaluation of pore occurrence in claddings manufactured with parameter set P1

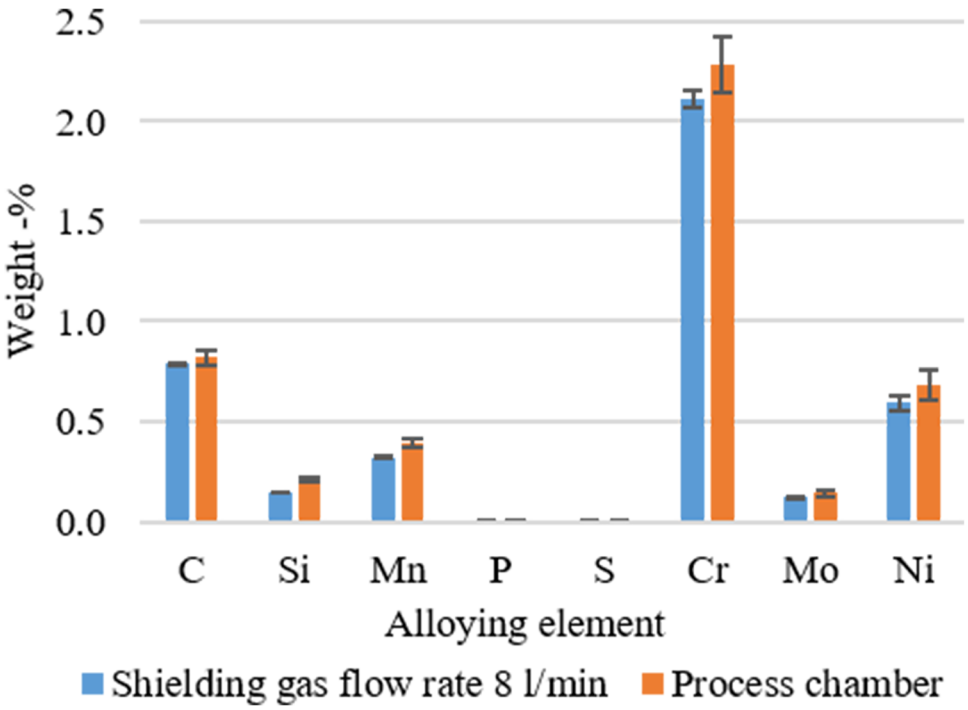

Fig. 11 Comparison of mean amount of alloying elements in claddings, shown with the confidence interval of the mean value, manufactured with 8 l/min argon gas flow rate and a process chamber (P1-S2)

sets with sparking (S1 & S2). A mean difference of 0.087% was found in those parameter sets. A spark spectrometer was used to determine the chemical composition of the claddings.

For parameter sets PS1 and PS2, the energy input during the LHWC processes outside the process chamber into the process zone was so high that the wire burned back and the process was prematurely terminated. An example of such a cladding is shown in Fig. 12.

For both sets of parameters, stabilization of the process was observed in the process chamber. The burn-back of the wire was considerably reduced. A wire burn-back occurred in the first two weld seams. A cladding with the same parameter set as in Fig. 12 but manufactured in the process chamber is shown in Fig. 13.

Hardness measurements were performed on claddings of parameter sets P1, P2, S1 and S2. Due to the partially unstable process with parameter set PS1 and PS2, a hardness measurement was not performed for these samples. High hardness values of 700 HV0.1 to 850 HV0.1 were found in the cladding of all samples, except for a cladding welded with parameter set P2 without process chamber. The comparison of the hardness curves of specimens welded with parameter set S1 in the process chamber and outside the process chamber is shown in Fig. 14. The mean hardness of the cladding welded in the process chamber is significantly higher than the cladding welded with an argon flow rate of 8 l/min in all cases. The base material has a hardness of 200 HV0.1.

The hardness profile of the specimens of parameter set P2 is shown in Fig. 15. Here, the significant difference of the hardness curves of the specimens welded in the chamber and outside the chamber is clearly visible. While a hardness of

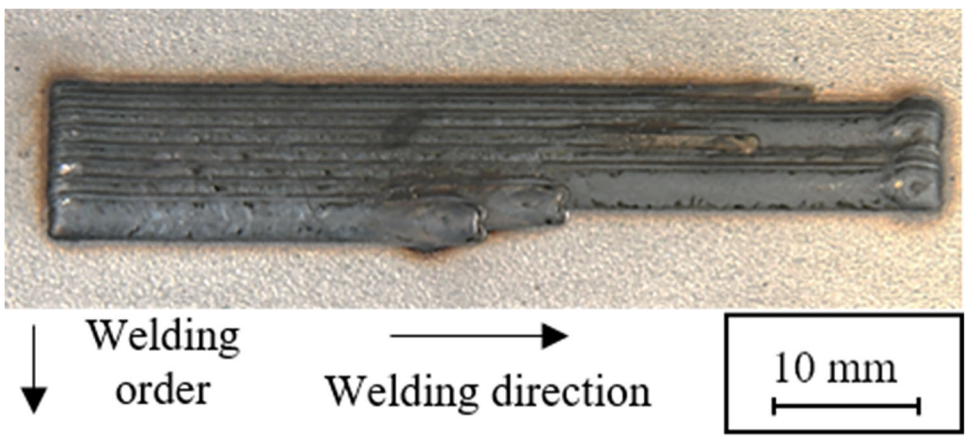

Fig. 12 Top view of a cladding manufactured outside of a process chamber, which was prematurely terminated due to a burned-back wire using welding parameter set PS1

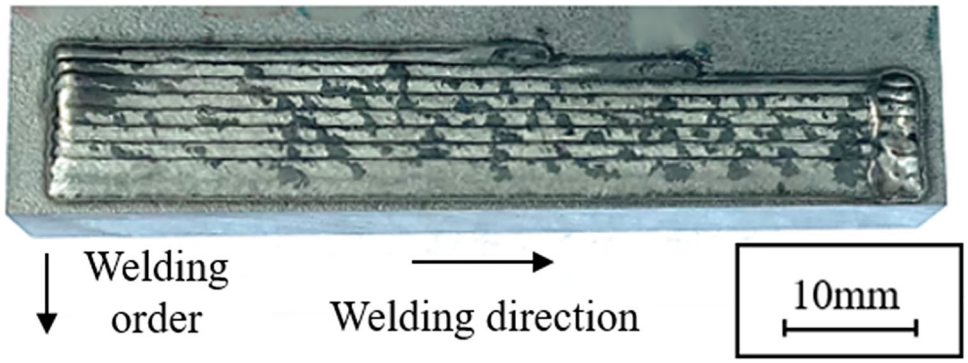

Fig. 13 Top view of a cladding manufactured in a process chamber using welding parameter set PS1

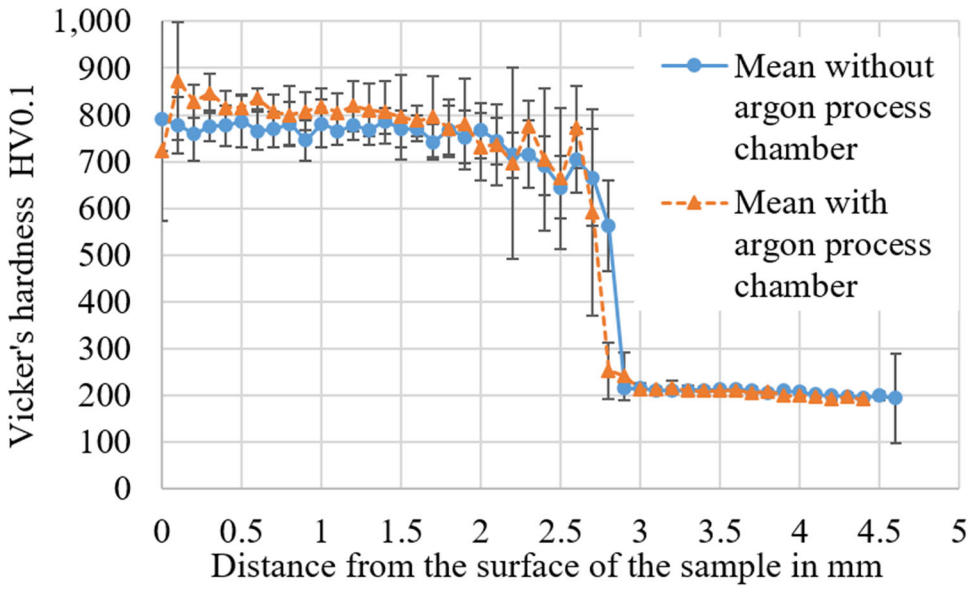

Fig. 14 Comparison of the hardness profile of claddings with parameter set S1, shown with the confidence interval of the mean value, in a process chamber and with an argon flow rate of 8 l/min

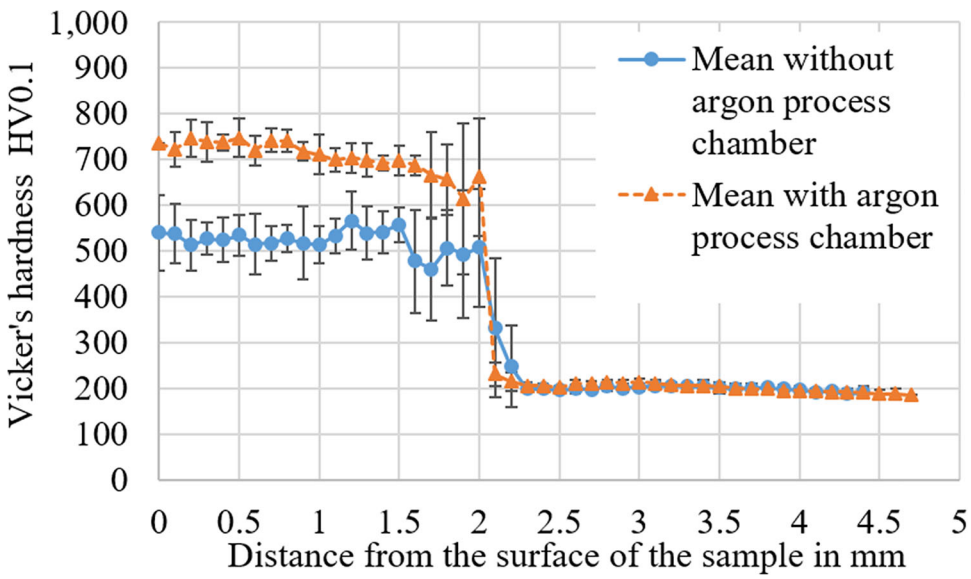

Fig. 15 Comparison of the hardness profile of claddings with parameter set P2, shown with the confidence interval of the mean value, in a process chamber and with an argon flow rate of 8 l/min

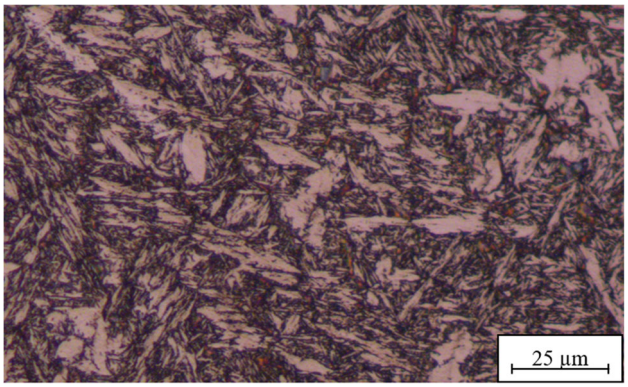

Fig. 16 Microstructure of a cladding of AISI 52100 with parameter set P2 in a process chamber

650 HV0.1 to 750 HV0.1 is achieved in the process chamber only a hardness of 480 HV0.1 to 540 HV0.1 is achieved outside the process chamber. The wire feed rate and the welding speed are identical in parameter sets P2 and S1. In parameter set P2, a higher laser power and a higher current intensity are used, which means that the applied energy and the energy per unit length are higher in parameter set P2. The lower hardness can be attributed to the higher dilution and the lower cooling rate due to the higher energy input.

As previously described, the cladding welded outside the process chamber with this set of parameters has a high dilution of about 25.9%. The sample welded in the process chamber, on the other hand, has a degree of dilution of only 11.0%. This is a possible explanation for the low hardness in the specimens welded outside the process chamber. In all samples, a martensitic microstructure is present. The microstructure is shown in Fig. 16.

Comparing the hardness values obtained with the investigations of Coors et al. [7], it is noticeable that the hardness values after cladding with a plasma transferred arc welding process are notably lower at 400 HV0.5 than the hardness values obtained in most claddings produced with LHWC. The reason for the difference in hardness is the high cooling rates during laser deposition welding. This leads to increased martensite formation and correspondingly higher hardness. Coors et al. were able to increase the hardness to a value of 880 HV0.5 in the cladding through subsequent forming and heat treatment. Such a post-treatment could possibly be dispensed with in the application of LHWC process.

4 Conclusion

In this study, it was demonstrated that the use of a process chamber flooded with argon affects the process stability and the chemical as well as mechanical properties of high carbon claddings. The following conclusions can be drawn:

- The dilution of the claddings manufactured in the process chamber is significantly lower than the dilution of claddings manufactured outside of the chamber. This indicates that the shielding gas coverage outside the chamber is not adequate for this material and that reaction of the melt pool with the ambient air occurs.
- During welding of AISI 52100 strong sparking occurs with some parameter sets. This effect can be suppressed by using a process chamber due to the suppressed oxidation.
- The process chamber leads to a reduction of pore occurrence, but not to a complete suppression of pore occurrence. The reason for the reduction has to be further investigated.
- The amount of alloying elements is higher in the claddings manufactured in a process chamber which indicates the burn-off of alloying elements during welding without the process chamber.
- The process chamber leads to a reduction of wire burnback and thereby increases process stability. This also suggests that a reaction of the melt pool with ambient air takes place outside the process chamber.
- High hardness values of 700 HV0.1 to 850 HV0.1 are achieved in most of the claddings. The increase in hardness of the cladding in the process chamber is statistically significant in all cases.

The results suggest that a process chamber and the associated improvement in shielding gas coverage can considerably increase the cladding quality. Since the use of a process chamber entails a more complex and less flexible design of the test setup, the next step should be to optimize the shielding gas coverage during welding outside the chamber to reproduce the conditions in the chamber. For this purpose, a determination of the shielding gas flow by means of Schlieren photography can be used to analyze and optimize the shielding gas flow.

Preheating of the substrate should also be considered in the simulation and design, as this is often used with high carbon steels to prevent cracking.

After improving the shielding gas coverage, investigations can be carried out to improve the cladding quality. The aim here is to achieve a defect-free cladding with a low level of dilution. The hardness values obtained in this and the previous investigation suggest that such a cladding can be used for application on highly loaded components, e.g., with rolling contact.

Author Contributions Conceptualization: L.B., T.C. Investigation: L.B., T.C., M.Y.F. Supervision: L.O., F.P., T.H. Visualization: L.B., K.B., T.C. Writing — original draft: L.B., K.B., T.C. Writing — review and editing: M.L., J.H., F.P., T.H., L.O.

Funding Open Access funding enabled and organized by Projekt DEAL. This research was funded by the Deutsche Forschungsgemeinschaft (DFG, German Research Foundation) - CRC 1153, subproject A4 -252662854.

Data Availability Data available on request from the authors

Code Availability Not applicable

Declarations

Conflict of interest The authors declare no competing interests.

References

1. Vilar R (1999) Laser alloying and laser cladding. Mater Sci Forum 301:229–252. https://doi.org/10.4028/www.scientific.net/MSF.301.229
2. Schuler V, Twrdek J (2019) Praxiswissen Schweisstechnik. Springer, Wiesbaden. https://doi.org/10.1007/978-3-658-24266-4, http://link.springer.com/10.1007/978-3-658-24266-4
3. Schulze G (2010) Die Metallurgie des Schweissens. Springer, Berlin Heidelberg, Berlin, Heidelberg. https://doi.org/10.1007/978-3-642-03183-0, http://link.springer.com/10.1007/978-3-642-03183-0
4. Sander J, Hufenbach J, Giebeler L, Wendrock H, Kühn U, Eckert J (2016) Microstructure and properties of FeCrMoVC tool steel produced by selective laser melting. Mater Des 89:335–341. https://doi.org/10.1016/j.matdes.2015.09.148
5. Kempen K, Vrancken B, Buls S, Thijs L, Van Humbeeck J, Kruth JP (2014) Selective laser melting of crack-free high density M2 high speed steel parts by baseplate preheating. J Manuf Sci Eng 136(6). https://doi.org/10.1115/1.4028513
6. Feuerhahn F, Schulz A, Seefeld T, Vollertsen F (2013) Microstructure and properties of selective laser melted high hardness tool steel. Physics Procedia 41:843–848. https://doi.org/10.1016/j.phpro.2013.03.157
7. Coors T, Mildebrath M, Büdenbender C, Saure F, Faqiri MY, Kahra C, Prasanthan V, Chugreeva A, Matthias T, Budde L, Pape F, Nürnberger F, Hassel T, Hermsdorf J, Overmeyer L, Breidenstein B, Denkena B, Behrens BA, Maier HJ, Poll G (2020) Investigations on tailored forming of AISI 52100 as rolling bearing raceway. Metals 10(10):1363. https://doi.org/10.3390/met10101363
8. Behrens BA, Maier HJ, Poll G, Overmeyer L, Wester H, Uhe J, Hassel T, Pape F, Lammers M, Hermsdorf J, Kaierle S, Budde L, Saure F, Mildebrath M, Coors T, Faqiri MY, Büdenbender C (2021) Influence of degree of deformation on welding pore reduction in high-carbon steels. Prod Eng 15(2):161–168. https://doi.org/10.1007/s11740-020-01009-z
9. Pape F, Coors T, Barroi A, Hermsdorf J, Mildebrath M, Hassel T, Kaierle S, Matthias T, Chugreev A, Chugreeva A, Behrens BA, Overmeyer L, Poll G (2018) Tribological study on tailored-formed axial bearing washers. Tribology Online 13(6):320–326. https://doi.org/10.2474/trol.13.320
10. Budde L, Prasanthan V, Merkel P, Kruse J, Faqiri MY, Lammers M, Kriwall M, Hermsdorf J, Stonis M, Hassel T, Breidenstein B, Behrens BA, Denkena B, Overmeyer L (2022) Material dependent surface and subsurface properties of hybrid components. Prod Eng. https://doi.org/10.1007/s11740-022-01128-9
11. Valiente Bermejo MA, Thalavai Pandian K, Axelsson B, Harati E, Kisielewicz A, Karlsson L (2021) Microstructure of laser metal deposited duplex stainless steel: Influence of shielding gas and heat treatment. Welding in the World 65(3):525–541. https://doi.org/10.1007/s40194-020-01036-5
12. Kampffmeyer D (2020) Tipps für die richtige Auswahl: Schutzgase zum Laserstrahlschweißen und - schneiden. Der Praktiker (10):500–503
13. Tapoglou N, Clulow J, Curtis D (2022) Increased shielding of a direct energy deposition process to enable deposition of reactive materials; an investigation into deposition of 15–5 PH stainless steel, Inconel 718 and Ti-6Al-4V. CIRP J Manuf Sci Technol 36:227–235. https://doi.org/10.1016/j.cirpj.2020.11.013
14. Pape F, Noelke C, Kaierle S, Haferkamp H, Gesing TM (2014) Influence of foaming agents on laser based manufacturing of closed-cell Ti foam. Procedia Mater Sci 4:97–102. https://doi.org/10.1016/j.mspro.2014.07.606
15. Guillen A, Goh F, Andre J, Barral A, Brochet C, Louis Q, Guillet T (2019) From the microstructure of steels to the explosion of sparks. Emergent Scientist 3:2. https://doi.org/10.1051/emsci/2019001
16. Budde L, Lammers M, Hermsdorf J, Kaierle S (2021) Process development for laser hot-wire deposition welding with high-carbon cladding Material AISI52100. In: Proceedings of LiM 2021
17. Lammers M, Hermsdorf J, Kaierle S, Ahlers H (2020) Entwicklung von Laser-Systemkomponenten für das koaxiale Laser-Draht-Auftragschweißen von Metall- und Glaswerkstoffen. In: Konstruktion für die Additive Fertigung 2019, Springer Berlin Heidelberg, Berlin, Heidelberg, pp 245–260. https://doi.org/10.1007/978-3-662-61149-4_15, http://link.springer.com/10.1007/978-3-662-61149-4_15
18. Kisielewicz A, Thalavai Pandian K, Sthen D, Hagqvist P, Valiente Bermejo MA, Sikström F, Ancona A (2021) Hot-wire laser-directed energy deposition: process characteristics and benefits of resistive pre-heating of the feedstock wire. Metals 11(4):634. https://doi.org/10.3390/met11040634
19. Pape F, Coors T, Matthias T, Behrens BA, Poll G (2020) Ultrasonic evaluation of tailored forming components. In: Bearing Steel Technologies: 12th Volume, Progress in Bearing Steel Metallurgical Testing and Quality Assurance, ASTM International, pp 300–312. https://doi.org/10.1520/STP162320190068, https://www.astm.org/doiLink.cgi?STP162320190068
20. Buzzard R (1933) The utility of the spark test as applied to commercial steels. Bur Stan J Res 11(4):527. https://doi.org/10.6028/jres.011.035
21. Schneider CA, Rasband WS, Eliceiri KW (2012) NIH Image to ImageJ: 25 years of image analysis. Nat Methods 9(7):671–675. https://doi.org/10.1038/nmeth.2089

Authors and Affiliations

Laura Budde[1] · Kai Biester[1] · Timm Coors[2] · Mohamad Yusuf Faqiri[3] · Marius Lammers[1] · Jörg Hermsdorf[1] · Thomas Hassel[3] · Florian Pape[2] · Ludger Overmeyer[1,4]

Kai Biester
k.biester@lzh.de

Timm Coors
coors@imkt.uni-hannover.de

Mohamad Yusuf Faqiri
faqiri@iw.uni-hannover.de

Marius Lammers
m.lammers@lzh.de

Jörg Hermsdorf
j.hermsdorf@lzh.de

Thomas Hassel
hassel@iw.uni-hannover.de

Florian Pape
pape@imkt.uni-hannover.de

Ludger Overmeyer
l.overmeyer@lzh.de

[1] Laser Zentrum Hannover e.V., Hollerithallee 8, Hannover 30419, Germany

[2] Leibniz University Hannover, Institute of Machine Design and Tribology, An der Universität 1, Garbsen 30823, Germany

[3] Leibniz University Hannover, Institute of Materials Science, An der Universität 2, Garbsen 30823, Germany

[4] Leibniz University Hannover, Institute of Transport and Automation Technology, An der Universität 2, Garbsen 30823, Germany